# Hydrophilic gold nanorods for biotechnological applications

Cite as: AIP Conference Proceedings **2416**, 020019 (2021); https://doi.org/10.1063/5.0069404
Published Online: 05 November 2021

**Iole Venditti, Annarita Stringaro, Marisa Colone, et al.**



# Hydrophilic Gold Nanorods for Biotechnological Applications

Iole Venditti[1,a)], Annarita Stringaro[2,b)], Marisa Colone[2,c)], Annarica Calcabrini[2,d)], Valentina Dini[3,e)], Giovanna Iucci[1,f)], Luca Tortora[1,4,g)], Martina Marsotto[1,h)] and Chiara Battocchio[1,i)]

[1]*Sciences Department, Roma Tre University, Via della Vasca Navale 79, 00146 Rome, Italy*
[2]*National Center for Drug Research and Evaluation, Istituto Superiore di Sanità, 00161 Rome, Italy*
[3]*National Center for Innovative Technologies in Public Health, Istituto Superiore di Sanità, 00161 Rome, Italy*
[4]*National Institute for Nuclear Physics – Roma Tre Division, via della Vasca Navale 84, 00146 Rome, Italy*

[a)] Corresponding author: iole.venditti@uniroma3.it
[b)] annarita.stringaro@iss.it
[c)] marisa.colone@iss.it
[d)] annarica.calcabrini@iss.it
[e)] valentina.dini@iss.it
[f)] giovanna.iucci@uniroma3.it
[g)] luca.tortora@uniroma3.it
[h)] martina.marsotto@uniroma3.it
[i)] chiara.battocchio@uniroma3.it

**Abstract.** Gold nanorods (AuNRs) are successfully employed in drug delivery, biosensors, and biotechnologies. Their wide success is due to their unique chemical properties, biocompatibility, easy, cheap and versatile synthesis. In this framework, AuNRs were synthetized with the aim to obtain strongly hydrophilic nanomaterials, suitable as drug delivery system. AuNRs were synthetized by seed mediated methods in two steps. After careful purification AuNRs were investigated by means of UV-Vis-NIR showing typical surface plasmon resonance (SPR) bands at 550 nm and 970 nm. The Fourier Transform Infrared Spectroscopy (FT-IR) and High-resolution X-ray photoelectron Spectroscopy (HR-XPS) investigations verified the surface functionalization by ascorbic acid (AA) and cetyl trimethyl ammonium bromide (CTAB) and allowed to examine the chemical structure and the interaction between capping agent and metal surface. Moreover, transmission electron microscopy (TEM) observations showed AuNRs with regular shape and size in the range of 20-80 nm. These results point to AuNRs as promising systems for drug delivery applications.

## INTRODUCTION

Inorganic materials and their composites have unique chemical and physical properties when they are nanosized and for this reason they are increasingly used in advanced devices for various fields of application, such as catalysis, energy, optoelectronics, biomedicine, and sensors [1-11]. Several recent achievements show the opportunity of producing new types of nanostructured materials with planned morphology, surface and desired properties [12–18].

Among other materials, gold nanorods (AuNRs) are specially being applied as biotechnological devices, in sensing platforms, in imaging/diagnostic tools and in drug delivery systems (see scheme in Fig.1).

*NanoInnovation 2020*
AIP Conf. Proc. 2416, 020019-1–020019-6; https://doi.org/10.1063/5.0069404
Published by AIP Publishing. 978-0-7354-4133-0/$30.00

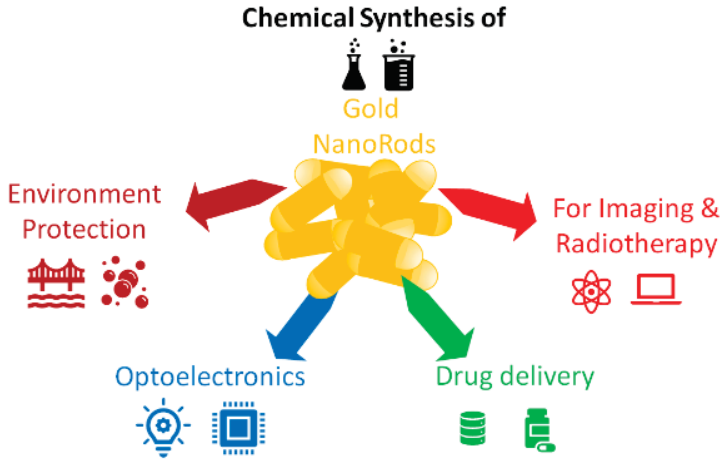


**FIGURE 1**. Scheme of main AuNRs biotechnological applications.

This widespread achievement is due to their modulable optical properties, biocompatibility, and versatile strategies for surface modification [19-22]. In fact, the modulable sizes make AuNRs active in the NIR, and this is very interesting specially in biomedical applications. The anisotropic shape, such as a rod, induces two bands of surface plasmon resonance (SPR). The first is a transverse plasmon band corresponding to an electron oscillation along the short axis of the rod, at around 520–550 nm. The second is a longitudinal plasmon band, in the range 800–1200 nm. The large use of AuNRs as biomedical therapeutic/imaging agents is due to this property, and the nanorods' aspect ratio can be tuned by the strict control of the experimental parameters during the chemical synthesis [23,24]. Furthermore, the presence of chemical or biological analytes can induce the aggregation, disaggregation or change of the local refractive index, which consequently generates changes of the LSPR band, and all this can be used in chemical sensing [25-27].

The mechanism of formation of AuNRs is still much debated because both thermodynamic and kinetic parameters come into play [24,28,29]. This expands the number of experimental parameters to consider, from the reagents concentrations, to the times, to pH, to temperature and so on. The final product, the rod, is also described by more properties than spherical nanoparticles. If for AuNPs only mean diameter and polydispersity are defined, AuNRs are described by aspect ratio, length, thickness, shape yield and reduction yield [30]. Among the various techniques to prepare AuNRs, the most widespread are the colloidal seed-mediated growth methods [19,31,32]. The principle is based first on the preparation of seeds of gold nanoparticles and then these are added to a growth solution: with the action of surfactants the seed crystals grow in an anisotropic way, forming gold rods with a certain aspect ratio. In some methods, silver nitrate is also added which helps and guides the anisotropic growth of the seeds. These methods yield good control of aspect ratio and above all good reproducibility allowing a wide range of applications such as biosensing, drug delivery and imaging [33-36].

In this framework, the synthesis of AuNRs was presented with the aim to obtain strongly hydrophilic anisotropic nanomaterials, suitable for drug delivery and photothermal therapy. AuNRs were synthetized by seed mediated methods in two steps and after careful purification they were investigated by means of UV-Vis-NIR Fourier Transform Infrared Spectroscopy (FT-IR) and Synchrotron Radiation induced X-ray Photoelectron Spectroscopy (SR-XPS). Moreover, Transmission Electron Microscopy (TEM) observations confirmed the nanosize in the range useful for biomedical applications.

# MATERIALS AND METHODS

## Materials

Gold (III) chloride hydrate (purity 99.9%), hexadecyltrimethylammonium bromide (purity 97 %) silver nitrate (purity 99.9%) and sodium borohydride ($NaBH_4$, purity 99.9%), were purchased from Merck. All the other products are regent grade and were used as received by Merck, without further purification.

## Instruments

UV-Vis-NIR spectra were collected in $H_2O$ solution by using a Nicolet™ iS50 FTIR Spectrometer (Thermo Scientific, USA), customized with Al optical coatings and multi-spectral range system (15 – 27,000 $cm^{-1}$).

SR-XPS measurements were carried out at the BACH (Beamline for Advanced DiCHroism) beamline at the ELETTRA facility in Trieste (Italy). The BACH beamline exploits the intense radiation emitted from an undulator front-end. XPS data were collected using a VG-Scienta R3000 hemispherical electron energy analyser in fixed angular mode (A21, pass energy = 50 eV), with the entrance and exit slits of the monochromator fixed at 30 μm and 20 μm, respectively. Photon energy of 360 eV was used for C1s and Au4f, spectral regions with a total binding energy resolution of 0.17 eV; for N1s and Ag3d spectral regions a photon energy value of 520 eV was selected, as to maximize signals intensities. The total binding energy resolution was about 0.22 eV. The energy scale was calibrated using as reference the C1s aliphatic signal at 285 eV and the Au4f7/2 signal of AuNRs arising by metallic gold atoms, always found at 83.96 eV. Curve-fitting analysis of the C1s, N1s, Au4f and Ag3d spectra was performed using Gaussian curves as fitting functions. Au4f7/2, Au4f5/2 and Ag3d5/2, Ag3d3/2 doublets were fitted by using the same full width at half-maximum (FWHM) for each pair of components of the same core level, a spin–orbit splitting of 6.0 eV and 3.7 eV respectively, and branching ratios Ag3d5/2/Ag3d3/2 = 3/2 and Au4f7/2/Au4f5/2 = 4/3. When several different species were individuated in a spectrum, the same FWHM value was used for all individual photoemission bands.

Electron microscopy analysis was carried out by a transmission electron microscope (Philips EM 208S –FEI, Company, Eindhoven, The Netherlands) with tungsten source and magnification power up to 200K, equipped with a MegaView III camera (Olympus Soft Imaging Solutions) for image acquisition. A drop of AuNRs suspension was placed onto a formvar–carbon-coated grid and then observed using TEM.

## AuNRs Synthesis

Synthesis involves two steps, in analogy with recent literature [19]: in the first the seed solution is prepared and then, in the second step, silver nitrate, auric tetrachloric acid, seed solution and ascorbic acid are mixed to grow the rods. The seed solution and the growth solution were prepared as follows. For the seed solution 5 mL of $HAuCl_4$ solution (0.0005 M) was added to 5 mL of CTAB solution (0.1 M) fluxed with Ar for 5 minutes and stirring rapidly (1200 rpm) at 25 °C. Then solution of $NaBH_4$ (0.01M) was prepared in ice cold water. 60 μL of this was injected rapidly to the gold−CTAB solution inducing a color change from pale yellow to brown-yellow. This was stirred at 1200 rpm for 2 min in ice cold water then was stirred 2 hours at 25°C. For the growth solution: 5 mL of $HAuCl_4$ solution (0.0010M) was added to 5 mL of CTAB solution (0.1M) followed by 50 μL of $AgNO_3$ solution (0.0004 M) stirring at 60 °C for 5 minutes. Then 70 μL of the ascorbic acid solution (0.08M) and subsequently 24 μL of seed solution were added; after 5 minutes the mixture was open and stirred at 25°C for 30 minutes and then purified by centrifugations (13000 rpm, 10 minutes, 2 times).

# RESULTS AND DISCUSSION

The synthesis is based on the seed mediated methods and the capping agents assure highly hydrophilia and possibility of size and size ratio modulation [19]. This is extremely important for drug delivery, AuNRs being able to act as a vehicle for biologically active but minimally hydrophilic and therefore minimally bioavailable molecules.

AuNRs synthesis involves two steps: in the first step the seed solution is prepared and then, in the second step, silver nitrate, auric tetrachloric acid, seed solution and ascorbic acid are mixed to grow the gold nanorods.

The AuNRs in water show two SPR bands: transverse and longitudinal (TrSPR and LgSPR). The plasmonic gold nanorod is more easily polarized longitudinally, meaning the SPR occurs at a lower energy, and thus higher wavelength. As the aspect ratio (ratio of length to width) of a nanorod is increased for a fixed diameter, the LgSPR and TrSPR are both affected; however, the longitudinal axis is more polarizable and more sensitive to aspect ratio changes. In AuNRs, the LgSPR wavelength can be tuned from 550 nm to over 2000 nm by adjusting to longer aspect ratios, while the TrSPR remains relatively constant at ~510 – 520 nm. It is reported in literature [37,38] that AuNRs can show a shift of few nanometers in the TrSPR absorption band (520 - 505 nm) induced by an increase in the aspect ratio from 1.7 to 5.2. On the other hand, the LgSPR can move from 590 nm to 935 nm when the aspect ratio increases from 1.7 to 5.2. In Figure 3, the UV-Vis-NIR spectrum in water confirmed AuNPs nanodimension and hydrophilia, showing typical TrSPR and LgSPR at 513 nm and 970 nm, respectively. For what regards their aspect ratio, the spectral features reported in Fig. 2 seem to be quite similar to the UV−Vis-NIR absorption spectra reported by Abidi and coworkers for gold NPs with a mean aspect ratio ranging from 3.7 to 5.2 [39].

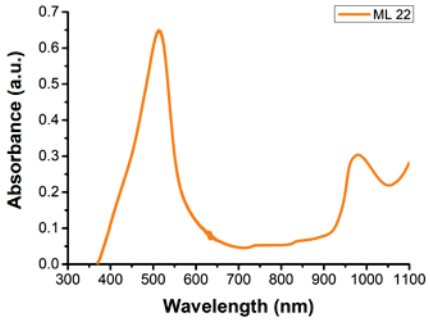


**FIGURE 2.** UV-Vis-NIR absorption spectrum of the synthesized AuNRs.

Transmission electron microscopy plays a key role in investigating nanomaterials' structures and linking properties associated with the nanoscale. In this case the TEM studies allow to observe AuNRs with size in the range of 20-80 nm. Figure 3a and 3b show some AuNRs with size of 20-35 nm.

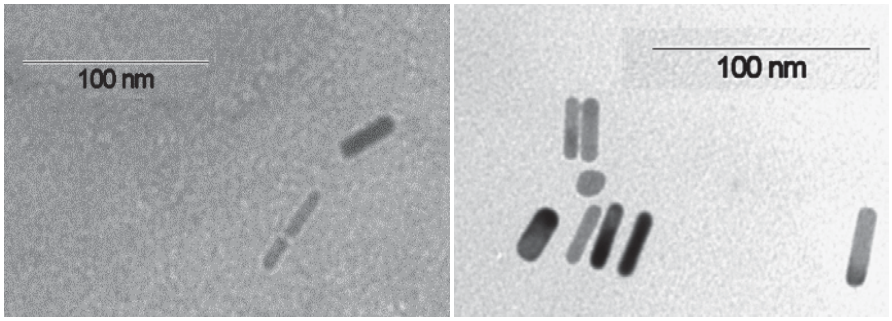


(a) (b)

**FIGURE 3.** TEM images of AuNRs.

In Fig. 4 some SR-XPS data were shown. SR-XPS analysis carried out at C1s, N1s, Au4f and Ag3d core levels confirmed the NRs chemical composition and allowed to assess the capping agent molecular stability. A very small amount of silver is observed, as expected by the synthetic procedure. Au4f signal has two components: the most intense spin-orbit pair is due to metallic gold atoms at the NR core, the signal at higher BE values is attributed to partially positively charged gold atoms at the NR surface. This behavior is similar to the one observed for gold nanoparticles stabilized by organic ligands [40].

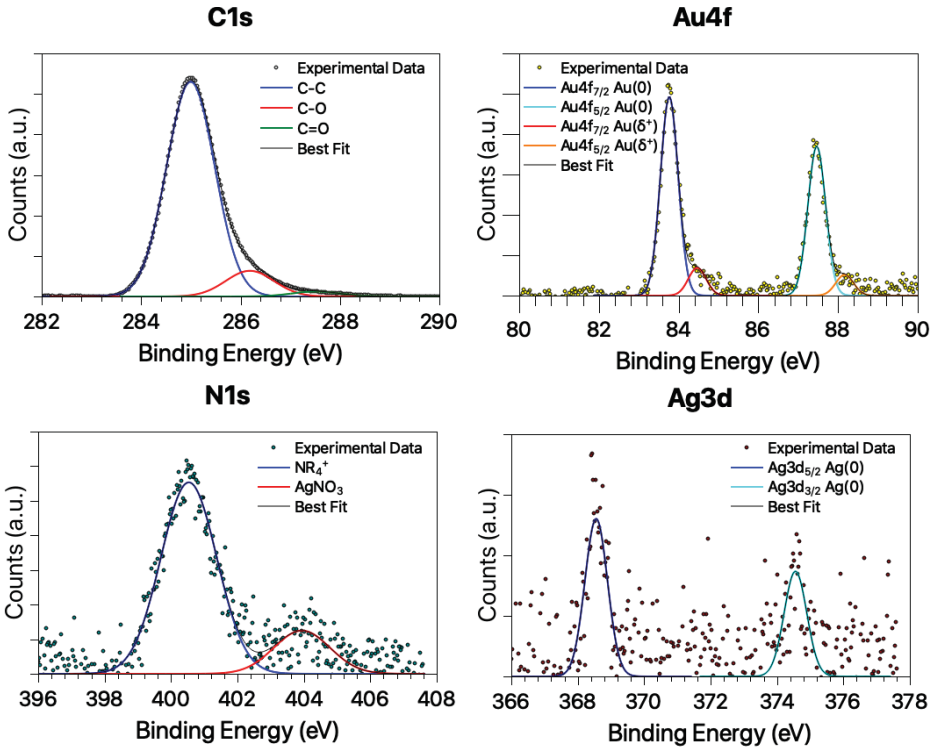


**FIGURE 4.** SR-XPS spectra collected at C1s, Au4f, N1s and Ag3d core levels on AuNRs.

## CONCLUSIONS

Hydrophilic AuNRs were synthesized and functionalized by AA and CTAB. SR-XPS investigations allowed to examine the chemical structure and the interaction between capping agents and metal surface. TEM studies showed AuNRs with size in the range of 20-80 nm.

These results show strongly hydrophilic and stable AuNRs as suitable and promising systems for drug delivery and photothermal therapy applications.

## ACKNOWLEDGMENTS

The Grant of Excellence Departments, MIUR (ARTICOLO 1, COMMI 314 – 337 LEGGE 232/2016), is gratefully acknowledged by authors of Roma Tre University. This research was partially funded by Istituto Superiore di Sanità, ISS (Ministry of Health - ISS funding).

## REFERENCES

1. Z. Zhang, W. Shen, J. Xue, Y. Liu, Y. Liu, P. Yan, and J. Liu, Nanoscale Res. Lett. **13**, 54 (2018).
2. S. Duan, Z. Du, H. Fan and R. Wang, Nanomaterials **8**, 949 (2018).
3. G. Naponiello, I. Venditti, V. Zardetto, D. Saccone, A. Di Carlo, I. Fratoddi, C. Barolo, and D. Dini, Appl. Surf. Sci. **356,** 911-920 (2015).
4. S. E. Lohse and C. J. Murphy, J. Am.Chem. Soc. **134**, 15607-15620 (2012).
5. I. Venditti, R. D'Amato, M.V. Russo, and M. Falconieri, Sens. Actuators B **126**, 35-40 (2007).
6. W. Zhang, M. Caldarola, X. Lu, B. Pradhan, and M. Orrit, Phys. Chem. Chem. Phys. **20**, 20468-20475 (2018).
7. I. Venditti, J. of King Saud University Science **31**, 398-411 (2019).
8. B. Zhou, J. Song, M. Wang, X. Wang, J. Wang, E. W. Howard, F. Zhou, J. Qu, and W. R. Chen, Nanoscale **10**, 21640-21647 (2018).

9. S. Pantalei, E. Zampetti, A. Macagnano, A. Bearzotti, I. Venditti, and M.V. Russo, Sensors **7**, 2920-2928 (2007).
10. C. D. Luo, Y. Y. Wang, X.M. Li, X. Q. Jiang, P. P. Gao, K. Sun, J.H. Zhou, Z. G. Zhang, and Q. Jiang, Nanomaterials **7**, 11 (2017).
11. D. Compagnone, G.C. Fusella, M. Del Carlo, P. Pittia, E. Martinelli, L. Tortora, R. Paolesse, and C. Di Natale, Biosens. Bioelectron. **42**, 618-625 (2013).
12. R. De Angelis, I. Venditti, I. Fratoddi, F. De Matteis, P. Prosposito, I. Cacciotti, L. D'Amico, F. Nanni, A. Yadav, M. Casalboni, and M. V. Russo, J. Colloid Interf. Sci. **414**, 24-32 (2014).
13. M. Swierczewska, K. Y. Choi, E. L. Mertz, X. Huang, F. Zhang, L. Zhu, H. Y. Yoon, and J. H. Park, Nano Lett. **12**, 3613-3620 (2012).
14. J. Chen, Y. Wang, C. Wang, R. Long, T. Chen, and Y. Yao, Chem. Commun. **55**, 6817-6826 (2019).
15. S. Huang, M. Bai and L. Wang, Sci. Rep. **3**, 2023 (2013).
16. K. Qi, R. Selvaraj, and L. Wang, Front. Chem. **8**, 616728 (2020).
17. W. A. Wani, S. Prashar, S. Shreaz, and S. Gómez-Ruiz, Coord. Chem. Rev. **312**, 67-98 (2016).
18. N. Labban, M. B. Wayu, C. M. Steele, T. S. Munoz, J. A. Pollock, W. S. Case, and M. C. Leopold, Nanomaterials **9**, 42 (2019).
19. K. Park, L. F. Drummy, R. C. Wadams, H. Koerner, D. Nepal, L. Fabris, and R. A. Vaia, Chem. Mater. **25**, 555-563 (2013).
20. Y. Yang, J. Zhang, F., Xia, C. Zhang, Q, Qian, X. Zhi, C. Yue, R. Sun, S. Cheng, S. Fang, W. Jin, Y. Yang, and D. Cui, Nanoscale Res. Lett. **11**, 285 (2016).
21. J. Perez-Juste, I. Pastoriza-Santos, L. M. Liz-Marzan, and P. Mulvaney, Coord. Chem. Rev., **249** 1870–1901 (2005).
22. H. Chen, L. Shao, Q. Lia, and J. Wang, Chem. Soc. Rev. **42**, 2679-2724 (2013).
23. I. Venditti, Bioengineering **6**, 53 (2019).
24. L. Scarabelli, A. Sánchez-Iglesias, J. Pérez-Juste and L. M. Liz-Marzán, J. Phys. Chem. Lett. **6**, 21, 4270-4279 (2015).
25. S. Prabhulkar, A. De la Zerda, A. Paranjape, and R. M. Awdeh, Biosensors **3**, 77-88(2013).
26. L. Vigderman, B. P. Khanal, and E. R. Zubarev, Adv. Mater. **24**, 4811-4841 (2012).
27. V. Pellas, D. Hu, Y. Mazouzi, Y. Mimoun, J. Blanchard, C. Guibert, M. Salmain, and S. Boujday, Biosensors **10**, 146 (2020).
28. Z. Wu, S. Yang, and W. Wu, Nanoscale **8**, 1237-1259 (2016).
29. N. Thomas and E. Mani, RSC Adv. **6**, 30028-30036 (2016).
30. R. Takahata, S. Yamazoe, K. Koyasu, K. Imura, and T. Tsukuda, J. Am. Chem. Soc. **140**, 6640–6647 (2018).
31. N. R. Jana, L. Gearheart, and C. J. Murphy, J. Physical Chem. B **105**, 4065-4067 (2001).
32. X. Ye, C. Zheng, J. Chen, Y. Gao, and C. B. Murray, Nano Letters **13**, 765-771 (2013).
33. H. Rao, X. Xue, H. Wang, and Z. Xue, J. Mater. Chem. C **7**, 4610-4621 (2019).
34. C. J. Murphy, H.-H. Chang, P. Falagan-Lotsch, M. T. Gole, D. M. Hofmann, K. N. L. Hoang, S. M. McClain, S. M. Meyer, J. G. Turner, M. Unnikrishnan, M. Wu, X. Zhang and Y. Zhang, Acc. Chem. Res. **52**, 2124-2135 (2019).
35. P. M. Lakhani, S. V. K. Rompicharla, B. Ghosh, and S. Biswas, Nanotechnology **26**, 432001 (2015).
36. L. Meng, J. Zhang, H. Li, W. Zhao, and T. Zhao, J. Nanomater. **2019**, 4925702 (2019).
37. R. Kumar, L. Binetti, T. Hien Nguyen, L. S. M. Alwis, A. Agrawal, T. Sun, and K. T.V. Grattan, Sci. Rep. **9**, 17469 (2019).
38. J. Wang, H. Z. Zhang, R. S. Li, and C. Z. Huang, TrAC Trac. Trends Anal. Chem. **80**, 429-443 (2016).
39. W. Abidi, P. R. Selvakannan, Y. Guillet, I. Lampre, P. Beaunier, B. Pansu, B. Palpant, and H. Remita, J. Phys. Chem. C **114**, 14794-14803 (2010).
40. I. Fratoddi, I. Venditti, C. Battocchio, L. Carlini, M. Porchia, F. Tisato, F. Bondino, E. Magnano, M. Pellei, C. Santini, Nanomaterials **9**, 772 (2019).